A Network Analogue Method for Computing the TEM Characteristics of Planar Transmission Lines

BENGT L. LENNARTSSON, STUDENT MEMBER, IEEE

Abstract—A network analogue method for calculation of the capacitance matrix of certain two-dimensional multiconductor systems is presented. The system is contained in a finite or infinite conducting rectangular boundary. An arbitrary number of parallel dielectric layers can be present, and the conductors consist of an arbitrary number of conducting strips at one or more of the dielectric interfaces. The strips are assumed to have zero thickness.

I. Introduction

UNDER THE QUASI-TEM assumption the different impedances and phase velocities for planar transmission lines can be calculated from the static capacitance matrix of the conductor system [1]. Hence the analysis is reduced to the problem of finding a solution of the two-dimensional Laplace's equation under the actual boundary conditions. In many cases, however, a complete solution of Laplace's equation is not necessary. If, for instance, a Green function can be found, this contains all the information needed for the derivation of the capacitance matrix. Bryant and Weiss [2] and Weeks [3] have computed a "dielectric Green function" from an integral equation. Yamashita and Atsuki [4] have derived trigonometric series expressions of a Green function for structures similar to those in Fig. 1. In this paper the capacitance matrix is obtained via an entirely different approach, the resistance network analogue. Network theory makes it possible to reduce a set of difference equations with millions of unknown potentials to a system of say one hundred variables and, moreover, network theory suggests ways to solve this latter system by direct methods.

II. Derivation of the Basic Matrix Relations

The five-point discrete Laplacian relates the potential at adjacent points in Fig. 2(a) according to (1).

$$\Phi_a + \Phi_b + \Phi_c + \Phi_d - 4\Phi_o = 0. \tag{1}$$

Equation (1) is also the node equation of node "o" in Fig. 2(b). Hence if any advantages can be obtained one may solve a network problem instead of the corresponding Laplace's difference equations. The potential distribution will be the same [5]. This idea has been used for simulation of boundaries on a network model, but also as a tool for a purely analytical approach [6].

Manuscript received November 10, 1971; revised February 10, 1972.

The author is with the Division of Network Theory, Chalmers University of Technology, Gothenburg, Sweden.

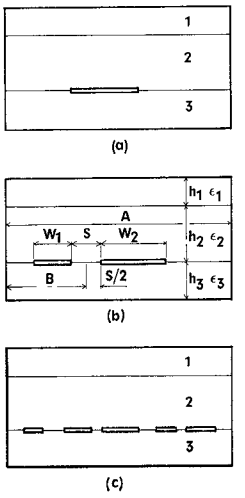

Fig. 1. Planar transmission lines, strips at one interface only.

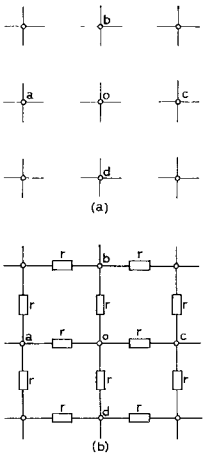

Fig. 2. The nodes of (a) the finite difference problem, and (b) the related network.

Now let us consider the networks in Fig. 3. The boundaries are at zero potential and the resistance and conductance matrices are $N \times N$. The definite terminal resistance matrix R_1 in Fig. 3(a) is simply $r_1 E$, where E is the $N \times N$ unit matrix, and the resistance of each resistor is r_1. In Fig. 3(b) a network has been connected in parallel to that in Fig. 3(a). The matrix G_1 is thus the sum of R_1^{-1} and the conductance matrix of the chain constituted by the elements g_1. From basic circuit theory we have

$$G_1 = R_1^{-1} + g_1 P \tag{2}$$

Authorized licensed use limited to: Linkoping Universitetsbibliotek. Downloaded on April 11,2010 at 19:38:04 UTC from IEEE Xplore. Restrictions apply.

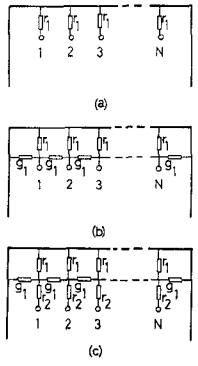

Fig. 3. Networks illustrating the recurrence relations (2) and (4).

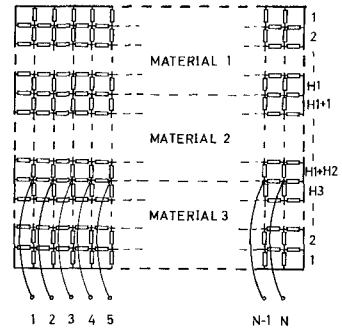

Fig. 4. A network analogue of the field problems in Fig. 1.

where P is the tri-diagonal matrix

$$P = \begin{vmatrix} 2 & -1 & 0 & - & - & - & - & 0 \\ -1 & 2 & -1 & 0 & & & & - \\ 0 & -1 & 2 & -1 & 0 & & & - \\ - & 0 & -1 & 2 & -1 & 0 & & - \\ \cdot & \cdot & \cdot & \cdot & \cdot & \cdot & \cdot & \cdot \\ \cdot & \cdot & \cdot & \cdot & \cdot & \cdot & \cdot & \cdot \\ - & & & & 0 & -1 & 2 & -1 \\ 0 & - & - & - & - & 0 & -1 & 2 \end{vmatrix}. \quad (3)$$

In Fig. 3(c) resistors r_2 are connected in series to each terminal of the network in Fig. 3(b). Hence

$$R_2 = G_1^{-1} + r_2 E = [R_1^{-1} + g_1 P]^{-1} + r_2 E. \quad (4)$$

The same procedure will be repeated when we connect a conductance chain g_2 in parallel, a set of resistors in series, etc. The recurrence relation can obviously be written

$$R_{k+1} = [R_k^{-1} + g_k P]^{-1} + r_{k+1} E \quad (5a)$$

where

$$R_1 = r_1 E. \quad (5b)$$

For the network analogue of the structures in Fig. 1 a proper choice of the network elements [5] is

$$g_k = \frac{1}{r_k} = \epsilon_r \quad (6a)$$

where $\epsilon_r = \epsilon_{r_1}$ for elements corresponding to material 1, etc., and

$$g_k = \frac{\epsilon_{r_1} + \epsilon_{r_2}}{2} \quad (6b)$$

at the interface between materials 1 and 2, etc. ϵ_{r_1}, ϵ_{r_2}, and ϵ_{r_3} are the equivalent relative dielectric constants of the materials.

Fig. 4 shows the network corresponding to the structures in Fig. 1. The matrix G_{tot} relates the potentials of the nodes at the lower interface to the currents entering these nodes, and G_{tot} can be decomposed according to

$$G_{tot} = \frac{\epsilon_{r_2} + \epsilon_{r_3}}{2} P + G_l + G_u \quad (7)$$

where the first term represents the chain at the interface, the second the network below, and the third the network above. G_l and G_u are obtained from (5) and (6). For instance, $G_u = R_k^{-1}$, where $k = H1 + H2$ and $G_l = R_{H3}^{-1}$ (Fig. 4). r_k and g_k are chosen according to (6). The matrix G_{tot} relates the terminal voltages to the terminal currents in Fig. 4.

In the following, the recurrence relation (5a) is transformed to diagonal form, and since inversion of a diagonal matrix just means inversion of its diagonal elements, the computing time can be reduced considerably.

III. Diagonalization of the Recurrence Relation

As P is symmetric, see (3), there is an orthogonal matrix A such that

$$A^* P A = \text{diag}\,(\lambda_1, \lambda_2, \cdots, \lambda_N) \quad (8a)$$

and

$$A^* A = E \quad (8b)$$

where the star denotes the transpose, and λ_i are the eigenvalues of P. The column vectors of A are the related normalized eigenvectors v_i. Analytic expressions for v_i and λ_i are known [7] and

$$\lambda_i = 4 \sin^2 \left[\frac{i\pi}{2(N+1)} \right] \quad (9)$$

$$(v_i)_j = \sqrt{\frac{2}{N+1}} \sin \left(\frac{ij\pi}{N+1} \right). \quad (10)$$

Thus

$$(A)_{i,j} = \sqrt{\frac{2}{N+1}} \sin \left(\frac{ij\pi}{N+1} \right). \quad (11)$$

From (5a) we now obtain by elementary matrix algebra

$$A^* R_{k+1} A = [(A^* R_k A)^{-1} + g_k \text{ diag } (\lambda_1, \lambda_2, \cdots, \lambda_N)]^{-1} + r_{k+1} E. \quad (12)$$

Since $R_1 = r_1 E$, it follows from (8b) that the right-hand side of (12) is diagonal for $k = 1$, and thus the left member is also diagonal for $k = 1$. Hence the right member is

Authorized licensed use limited to: Linkoping Universitetsbibliotek. Downloaded on April 11,2010 at 19:38:04 UTC from IEEE Xplore. Restrictions apply.

diagonal for $k=2$, and from mathematical induction it now follows that A^*R_kA is diagonal for each k. If we introduce the vector $(\alpha^k)_i$ according to

$$(\alpha^k)_i = (A^*R_kA)_{i,i}, \qquad i = 1, 2, \cdots, N \tag{13}$$

we can replace the matrix relation (5) by the much simpler vector relation

$$(\alpha^{k+1})_i = \frac{1}{\dfrac{1}{(\alpha^k)_i} + g_k\lambda_i} + r_{k+1}, \qquad i = 1, 2, \cdots, N \tag{14a}$$

where

$$(\alpha^1)_i = r_1, \qquad i = 1, 2, \cdots, N. \tag{14b}$$

If $H1$ or $H3$ in Fig. 4 is infinite, it is easy to obtain the limit as $k \to \infty$ in (14a).

As an analytical expression for the eigenvalues λ_i of P is known, (14) are now well prepared for computer work. It remains to compute G_{tot} (7), or better its inverse R_{tot}. That is done in the following way.

1) Let the computer perform (14) for $k=1, 2, \cdots, H1+H2-1$. r_k and g_k are obtained from (6a) and (6b). For convenience let us denote the resulting vector of this procedure D_u.

2) Let the computer perform (14) for $k=1, 2, \cdots, H3-1$, where r_k and g_k are chosen according to (6a). Denote the resulting vector D_l.

The elements of the matrix $R_{tot}=G_{tot}^{-1}$ are now according to the Appendix obtained from

$$(R_{tot})_{i,j} = F(i-j) - F(i+j) \tag{15}$$

where

$$F(m) = \frac{1}{N+1}\sum_{k=1}^{N} \frac{\cos\left(\dfrac{mk}{N+1}\right)}{\dfrac{\epsilon_{r_2}+\epsilon_{r_3}}{2}\lambda_k + (D_u)_k + (D_l)_k}. \tag{16}$$

The auxiliary vector F has been introduced to achieve further reduction of computing time and storage requirements (see Appendix).

IV. Derivation of the Capacitance Matrix

As we now have computed the definite terminal resistance matrix R_{tot} for the network in Fig. 4, we have a simple model for this network, Fig. 5.

Next we introduce the conducting strips at the interface between materials 2 and 3 in Figs. 1 and 4. The matrix R_{tot} itself is unaffected by the number of strips, their widths, and separations. Consider, for instance, the coupled microstrip in Fig. 1(b). Let the left-hand strip cover the nodes with indices from k_1 to k_2 and the right-hand strip the nodes from k_3 to k_4 in Figs. 4 and 5. Let V_A denote the potential of the left-hand strip and V_B the potential of the right-hand one. The injected currents and voltages in Figs. 4 and 5 should in this case be chosen such that

$$V_i = V_A, \quad \text{for } k_1 \le i \le k_2$$
$$V_i = V_B, \quad \text{for } k_3 \le i \le k_4$$
$$I_i = 0, \quad \text{for } 1 \le i < k_1,\ k_2 < i < k_3, \text{ and } k_4 < i \le N.$$

Thus we get

$$\begin{bmatrix} V_1 \\ V_2 \\ \vdots \\ V_{k_1-1} \\ \hline V_A \\ \vdots \\ V_A \\ \hline V_{k_2+1} \\ \vdots \\ \hline V_B \\ \vdots \\ V_B \\ \hline V_{k_4+1} \\ \vdots \\ V_N \end{bmatrix} = \begin{bmatrix} (R_{tot})_{1,1} & \cdots & \cdots & \cdots & \cdots \\ \vdots & & & & \\ \vdots & & & & \\ \vdots & & & & \\ \hline \vdots & & & & \\ \vdots & & & & \\ \vdots & & & & \\ \hline \vdots & & & & \\ \vdots & & & & \\ \hline \vdots & & & & \\ \vdots & & & & \\ \vdots & & & & \\ \hline \vdots & & & & \\ \vdots & & & & \\ \vdots & & & & \end{bmatrix} \begin{bmatrix} 0 \\ 0 \\ \vdots \\ 0 \\ \hline I_{k_1} \\ \vdots \\ I_{k_2} \\ \hline 0 \\ \vdots \\ \hline I_{k_3} \\ \vdots \\ I_{k_4} \\ \hline 0 \\ \vdots \\ 0 \end{bmatrix}. \tag{17}$$

Authorized licensed use limited to: Linkoping Universitetsbibliotek. Downloaded on April 11,2010 at 19:38:04 UTC from IEEE Xplore. Restrictions apply.

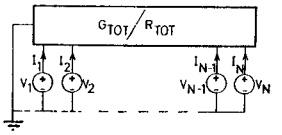

Fig. 5. Definite conductance/resistance matrix model of the network in Fig. 4.

As we have no interest in the potential of the nodes outside the strips, we can omit rows and columns of R_{tot} corresponding to such nodes. Let the remaining part of R_{tot} (shadowed in (17)) constitute a new matrix R_{red}. Then we have

$$\begin{bmatrix} V_A \\ V_A \\ \vdots \\ V_A \\ -- \\ V_B \\ \vdots \\ V_B \end{bmatrix} = \left[\begin{array}{ccc|c} (R_{red})_{1,1} & \cdots & & \cdots \\ & & & \\ & & & \\ & & & \\ \hline & & & \end{array}\right] \begin{bmatrix} I_{k_1} \\ I_{k_1+1} \\ \vdots \\ I_{k_2} \\ -- \\ I_{k_3} \\ \vdots \\ I_{k_4} \end{bmatrix}. \quad (18)$$

Obviously there is no reason to compute the elements of R_{tot} that do not occur in R_{red}. Let G_{red} denote the inverse of R_{red}, i.e.,

$$\begin{bmatrix} I_{k_1} \\ I_{k_1+1} \\ \vdots \\ I_{k_2} \\ -- \\ I_{k_3} \\ \vdots \\ I_{k_4} \end{bmatrix} = \left[\begin{array}{ccc|c} (G_{red})_{1,1} & \cdots & & \cdots \\ & & & \\ & & & \\ & & & \\ \hline & & & \end{array}\right] \begin{bmatrix} V_A \\ V_A \\ \vdots \\ V_A \\ -- \\ V_B \\ \vdots \\ V_B \end{bmatrix}. \quad (19)$$

R_{red} is a definite resistance terminal matrix, and it is thus necessarily symmetric and positive definite. The method of inversion due to Cholesky may therefore be suitable [8]. The Cholesky routines SINV and DSINV are available in Fortran SSP [9]. SINV has been used by the author on an IBM 360/65 computer, and 50×50 matrices, for instance, were inverted in about 2 s.

Let the total currents entering the networks in Figs. 4 and 5 from the left- and right-hand strip be I_A and I_B, respectively, that is

$$I_A = \sum_{k=k_1}^{k_2} I_k \quad (20a)$$

and

$$I_B = \sum_{k=k_3}^{k_4} I_k. \quad (20b)$$

From (19) we can easily see that

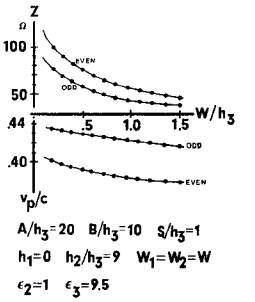

Fig. 6. Impedances and relative phase velocities versus strip width for the structure in Fig. 1(b) from the author's program (ooo), and according to Judd *et al.* [10] (———).

$$I_A = g_{11}V_A + g_{12}V_B \quad (21a)$$

and

$$I_B = g_{21}V_A + g_{22}V_B \quad (21b)$$

where g_{11} is the sum of the elements of the upper left submatrix of G_{red} in (19), g_{12} is the sum of the elements of the upper right submatrix, etc. As G_{red} is symmetric, $g_{12} = g_{21}$.

Let us now leave network theory and return to the field problem. Q_A and Q_B are the charges per unit length for the left- and right-hand strip, respectively. Then we have

$$Q_A = c_{11}V_A + c_{12}V_B \quad (22a)$$

and

$$Q_B = c_{21}V_A + c_{22}V_B. \quad (22b)$$

From the choice of the network elements (6) it follows [5] that the relation between the coefficients of (21) and (22) is

$$c_{ij} = \epsilon_0 g_{ij}. \quad (23)$$

V. Discussion

The TEM parameters can easily be obtained from the capacitance matrix [1]. The algorithm presented in this paper has been used for design of nonsymmetrical coupled microstrip in power dividers and of single microstrip with satisfactory results. In special case, coupled microstrip, it has been compared with the method due to Judd *et al.* [10]. The differences between the two methods in impedances and phase velocities were overall less than 1 percent, see Fig. 6. Three types of errors have to be considered: errors due to the TEM assumption, roundoff errors, and errors due to the introduction of the discrete Laplacian. The TEM theory is exact for low frequencies and the error is of the order of a few percent at 5 GHz [11]. The second type of error is quite negligible. The author has found that 2–3 significant digits were lost, when a 7-digit representation was used. The errors in the impedances due to the introduction of the discrete five-point Laplacian have turned out to be of the order h^1, where h is the node separation. The author has used an h^1 extrapolation in some cases.

Authorized licensed use limited to: Linkoping Universitetsbibliotek. Downloaded on April 11,2010 at 19:38:04 UTC from IEEE Xplore. Restrictions apply.

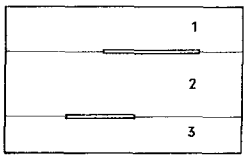

Fig. 7. A structure having strips at two interfaces.

When the order of G_{tot} was 1000–6000, and the order of G_{red} 60–100, this h^1 error was less than 2 percent. (The h^1 error always tends to make the computed impedances less than the correct values.)

In this paper only the structure of Fig. 1(b) has been considered. However, very little modification is needed for the analysis of the structures in Fig. 1(a) and 1(c). Three dielectrics are present, but as long as the interfaces are parallel planes, the number of dielectrics is arbitrary. For the structure in Fig. 7 the recurrence relation (5) has to be slightly modified. The matrices will be $2N\times 2N$ but can easily be transformed to a form, where only diagonal submatrices of order $N\times N$ have to be inverted.

Appendix

We have the relation

$$G_{\text{tot}} = \frac{\epsilon_{r_2} + \epsilon_{r_3}}{2} P + G_u + G_l \tag{7}$$

where

$$G_u = A D_u A^* \tag{A1a}$$

and

$$G_l = A D_l A^*. \tag{A1b}$$

From (11) we can see that A is symmetric, and hence the star denoting the transpose can be omitted, that is $A = A^* = A^{-1} = (A^*)^{-1}$. From (A1) we then have $AG_uA = D_u$ and $AG_lA = D_l$, and multiplications of (7) from left and right by A yield

$$AG_{\text{tot}}A = \frac{\epsilon_{r_2} + \epsilon_{r_3}}{2} APA + AG_uA + AG_lA$$

$$= \operatorname*{diag}_{i=1,N}\left[\frac{\epsilon_{r_2} + \epsilon_{r_3}}{2}\lambda_i + (D_u)_i + (D_l)_i\right]$$

or

$$G_{\text{tot}} = A \operatorname*{diag}_{i=1,N}\left[\frac{\epsilon_{r_2} + \epsilon_{r_3}}{2}\lambda_i + (D_u)_i + (D_l)_i\right] A.$$

This can be inverted to

$$R_{\text{tot}} = A \operatorname*{diag}_{i=1,N}\left[\frac{1}{\frac{\epsilon_{r_2} + \epsilon_{r_3}}{2}\lambda_i + (D_u)_i + (D_l)_i}\right] A.$$

Let us for a moment introduce

$$d_{i,i} = \frac{1}{\frac{\epsilon_{r_2} + \epsilon_{r_3}}{2}\lambda_i + (D_u)_i + (D_l)_i}.$$

Then

$$(R_{\text{tot}})_{i,j} = \sum_{k=1}^{N} (A)_{i,k} d_{k,k} (A)_{k,j}. \tag{A2}$$

From (11) and (A2) we now obtain

$$(R_{\text{tot}})_{i,j} = \frac{2}{N+1}\sum_{k=1}^{N} d_{k,k} \sin\left(\frac{ik\pi}{N+1}\right)\sin\left(\frac{jk\pi}{N+1}\right)$$

$$= \frac{1}{N+1}\sum_{k=1}^{N} d_{k,k}\left[\cos\frac{(i-j)k\pi}{N+1} - \cos\frac{(i+j)k\pi}{N+1}\right]$$

and if

$$F(m) = \frac{1}{N+1}\sum_{k=1}^{N} \frac{\cos\left(\frac{mk\pi}{N+1}\right)}{\frac{\epsilon_{r_2} + \epsilon_{r_3}}{2}\lambda_k + (D_u)_k + (D_l)_k} \tag{16}$$

we have

$$(R_{\text{tot}})_{i,j} = F(i-j) - F(i+j). \tag{15}$$

As mentioned above, the elements of F and R_{tot} have to be calculated only for indices occurring in the reduced matrix R_{red}.

Acknowledgment

The author wishes to thank Prof. E. F. Bolinder and R. Ekinge for helpful discussions during the course of this work.

References

[1] M. A. R. Gunston and J. R. Weale, "The transmission characteristics of microstrip," *The Marconi Rev.* (GB), vol. 32, pp. 226–243, Oct.–Dec. 1969.
[2] T. G. Bryant and J. A. Weiss, "Parameters of microstrip transmission lines and coupled pairs of microstrip lines," *IEEE Trans. Microwave Theory Tech.*, vol. MTT-16, pp. 1021–1027, Dec. 1968.
[3] W. T. Weeks, "Calculation of coefficients of capacitance of multiconductor transmission lines in the presence of a dielectric interface," *IEEE Trans. Microwave Theory Tech.*, vol. MTT-18, pp. 35–43, Jan. 1970.
[4] E. Yamashita and K. Atsuki, "Strip line with rectangular outer conductor and three dielectric layers," *IEEE Trans. Microwave Theory Tech.*, vol. MTT-18, pp. 238–244, May 1970.
[5] G. Liebmann, "Solution of partial differential equations with a resistance network analogue," *British J. Appl. Phys.*, vol. 1, pp. 92–103, Apr. 1950.
[6] K. F. Sander, "The application of network analysis to the resistance network analogue and to relaxation procedures," *Proc. Inst. Elec. Eng.*, vol. 109-C, pp. 516–526, Sept. 1962.

Authorized licensed use limited to: Linkoping Universitetsbibliotek. Downloaded on April 11,2010 at 19:38:04 UTC from IEEE Xplore. Restrictions apply.

[7] R. T. Gregory and D. L. Karney, *A Collection of Matrices for Testing Computational Algorithms*. New York: Wiley, 1969, p. 137.
[8] J. Westlake, *A Handbook of Numerical Matrix Inversion and Solution of Linear Equations*. New York: Wiley, 1968, pp. 106–107.
[9] *System/360 Scientific Subroutine Package, Version III*, IBM Appl. Progr. H20-0205-03, IBM, 1968.
[10] S. V. Judd, I. Whiteley, R. J. Clowes, and D. C. Rickard, "An analytical method for calculating microstrip transmission line parameters," *IEEE Trans. Microwave Theory Tech.*, vol. MTT-18, pp. 78–87, Feb. 1970.
[11] P. Troughton, "Measurement techniques in microstrip," *Electron. Lett.*, vol. 5, pp. 25–26, Jan. 1969.

Dynamic Behavior of Nonlinear Power Amplifiers in Stable and Injection-Locked Modes

YOICHIRO TAKAYAMA

***Abstract*—Dynamic equations of reflection-type nonlinear power amplifiers in both stable and injection-locked modes are derived for modulated signals. The steady-state response and the transient response of an injection-locked negative-resistance diode amplifier is evaluated. The response for an FM signal is discussed. Numerical results show that the dynamic behavior as well as the steady-state behavior is affected by nonlinearity of the diode conductance and susceptance.**

Introduction

MICROWAVE power amplifiers, including injection-locked ones, using new negative-resistance diodes such as IMPATT diodes and Gunn effect diodes, have been investigated in recent years. Steady-state single-frequency responses of nonlinear power amplifiers in both stable[1] and injection-locked modes have been investigated theoretically and experimentally by several authors [1]–[3]. Nonlinear effects are expected not only in the steady-state behavior but also in the dynamic behavior. The dynamic behavior of injection-locked oscillators or amplifiers was studied, so far, following Adler's theory [4]. More recently, Kuno *et al.* [5] have presented amplitude and phase equations evolved by using the nonlinear instantaneous voltage-controlled device model.

The present purpose is to investigate nonlinear admittance effects on both steady-state and dynamic behaviors of nonlinear power amplifiers. Dynamic equations for reflection-type nonlinear power amplifiers in both stable and injection-locked modes were derived for modulated signals by extending the results evolved from the method of expansion of the injection-locked oscillator admittance [2], [6]–[8]. The steady-state responses and the transient responses of an injection-locked amplifier were evaluated by sample calculations on the simplified model of a negative-resistance diode amplifier. The response for an FM signal is also discussed.

Manuscript received November 18, 1971; revised January 28, 1972.
The author is with Central Research Laboratories, Nippon Electric Co., Ltd., Kawasaki, Japan.
[1] "Stable mode" is amplification mode where oscillation will not occur if undriven.

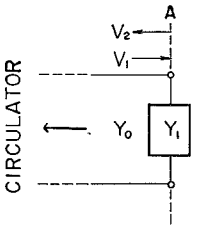

Fig. 1. Reflection-type amplifier diagram.

Dynamic Equations

The reflection-type amplifier uses a circulator to provide input–output isolation. The basic network used for analysis is shown in Fig. 1, where V_1 and V_2 are the incident and reflected voltage waves at reference plane A. The active network (whose admittance is Y_1), including the negative-resistance diode, is connected to a matched circulator through the lossless transmission line with characteristic admittance Y_0.

V_1 and the ac voltage V_3 across Y_1, which are sinusoidal with slowly varying amplitude and phase, can be expressed by

$$V_1 = \tilde{V}_1(t)e^{j(\omega t+\alpha(t))}$$
$$V_3 = \tilde{V}_3(t)e^{j(\omega t+\theta(t))} \quad (1)$$

Authorized licensed use limited to: Linkoping Universitetsbibliotek. Downloaded on April 11,2010 at 19:38:04 UTC from IEEE Xplore. Restrictions apply.